3-2009

Dynamical and Precipitation Structures of Poleward-Moving Tropical Cyclones in Eastern Canada, 1979-2005

Shawn M. Milrad
McGill University, milrads@erau.edu

Eyad H. Atallah
McGill University

John R. Gyakum
McGill University

Scholarly Commons Citation

Milrad, S. M., Atallah, E. H., & Gyakum, J. R. (2009). Dynamical and Precipitation Structures of Poleward-Moving Tropical Cyclones in Eastern Canada, 1979-2005. *Monthly Weather Review, 137*(3). https://doi.org/10.1175/2008MWR2578.1

Dynamical and Precipitation Structures of Poleward-Moving Tropical Cyclones in Eastern Canada, 1979–2005

SHAWN M. MILRAD, EYAD H. ATALLAH, AND JOHN R. GYAKUM

Department of Atmospheric and Oceanic Sciences, McGill University, Montreal, Quebec, Canada

(Manuscript received 28 February 2008, in final form 5 September 2008)

ABSTRACT

Tropical cyclones in the western North Atlantic basin are a persistent threat to human interests along the east coast of North America. Occurring mainly during the late summer and early autumn, these storms often cause strong winds and extreme rainfall and can have a large impact on the weather of eastern Canada. From 1979 to 2005, 40 named (by the National Hurricane Center) tropical cyclones tracked over eastern Canada. Based on the time tendency of the low-level (850–700 hPa) vorticity, the storms are partitioned into two groups: ''intensifying'' and ''decaying.'' The 16 intensifying and 12 decaying cases are then analyzed using data from both the National Centers for Environmental Prediction (NCEP) North American Regional Reanalysis (NARR) and the NCEP global reanalysis. Composite dynamical structures are presented for both partitioned groups, utilizing both quasigeostrophic (QG) and potential vorticity (PV) perspectives. It is found that the proximity to the tropical cyclone and subsequent negative tilt (or lack thereof) of a precursor trough over the Great Lakes region is crucial to whether a storm ''intensifies'' or ''decays.'' Heavy precipitation is often the main concern when tropical cyclones move northward into the midlatitudes. Therefore, analyses of storm-relative precipitation distributions show that storms intensifying (decaying) as they move into the midlatitudes often exhibit a counterclockwise (clockwise) rotation of precipitation around the storm center.

1. Introduction

a. Motivation

Occurring mainly during the late summer and early autumn, tropical cyclones that move poleward and affect the midlatitudes of the North Atlantic basin can have a large impact on the weather of eastern Canada, especially in terms of extreme rainfall events. Operational forecasters in the region face a major challenge (Fogarty 2002b) in predicting extratropical transitions (ETs) of tropical cyclones in eastern Canada, which occur 1–2 times per year on average (Hart and Evans 2001). The exact location of impact, ranging from southern Ontario to eastern Newfoundland, varies based on several factors (e.g., season, sea surface temperature, track, and synoptic situation).

In 2005, the remnants of Hurricanes Katrina and Rita were responsible for a significant percentage of the total monthly precipitation throughout a large portion of the St. Lawrence River Valley and eastern Canada. For example, 55% (73 mm) of the total August 2005 precipitation at Montreal (YUL) fell on one day (31 August), in association with the remnants of Katrina. In September of the same year, Stephenville, Newfoundland, received 151.4 mm (54% of the total September 2005 precipitation) of precipitation due to the northward-moving remnants of Hurricane Rita. To provide perspective on how extreme these rainfall values are, the average precipitation for the entire month of August in Montreal is 92.7 mm; while at Stephenville, Newfoundland, the average precipitation received for the month of September is 128 mm.

The work of Hart and Evans (2001) is the most complete (1899–1996) ET climatology in the Atlantic basin, showing that 50% of landfalling tropical cyclones in the western Atlantic are storms that have undergone or are undergoing extratropical transition. During the period from 1979 to 1993, they show that 46% of Atlantic tropical cyclones undergo ET at some point during their life cycle. Moreover, of the 61 transitioning tropical cyclones that they marked from 1979 to 1993, 51% experience posttransition intensification. In addition, they find a latitudinal dependence whereby 60% of

Corresponding author address: Shawn M. Milrad, Dept. of Atmospheric and Oceanic Sciences, McGill University, 805 Sherbrooke St. West, Montreal QC H3A 2K6, Canada.
E-mail: shawn.milrad@gmail.com

DOI: 10.1175/2008MWR2578.1

tropical cyclones that undergo post-ET intensification have a point of origin south of 20°N. In contrast, 90% of tropical cyclones that weaken post-ET originate north of 20°N. This suggests that baroclinic characteristics in the initial tropical vortex may not be conducive to a strong ET later in the storm's lifetime (Hart and Evans 2001).

An integral part of the Hart and Evans (2001) Atlantic climatology is the seasonal dependence of ET occurrence. As shown by Hart and Evans, the probability of a storm undergoing ET in the North Atlantic increases as the tropical cyclone season progresses. In addition, their findings indicate that ET typically occurs at lower latitudes at the beginning and the end of the season and at higher latitudes during peak season. This is primarily due to the delayed warming of the Atlantic, which allows tropical systems to survive as purely tropical entities at higher latitudes during the month of September (Hart and Evans 2001). Similar climatologies have been performed for other tropical cyclone basins, most notably the western North Pacific (Klein et al. 2000) and the eastern Indian Ocean (Foley and Hanstrum 1994).

There have been numerous case studies performed with regard to these storms in recent years. A particularly prominent major flooding event in the northeast United States and eastern Canada, the remnants of Hurricane Hazel in 1954 (Palmén 1958; Matano 1958; Anthes 1990; Weese 2003; Gyakum 2003), helped inspire the first in-depth studies of ET. Recent research focuses on either the western North Pacific basin (Matano and Sekioka 1971a,b; Harr and Elsberry 2000; Harr et al. 2000; Klein et al. 2000; Ritchie and Elsberry 2003; Elsberry 2002; Klein et al. 2002), western Europe (Thorncroft and Jones 2000; Browning et al. 1998; Agusti-Panareda et al. 2004; Browning et al. 2000), or the United States (DiMego and Bosart 1982a,b; Atallah and Bosart 2003; Bosart and Dean 1991; Colle 2003; Carr and Bosart 1978; Dickinson et al. 2004).

Two published works with major relevance to this paper are Hart et al. (2006) and Ritchie and Elsberry (2007). In Hart et al. (2006), 34 cases of storms that are undergoing ET are examined and partitioned based on an intensification criterion (this is discussed more in-depth in section 3a). Hart et al. (2006) state that the "determination of whether a cyclone will undergo intensification or decay post-ET is critical to accurate forecasting of the storm-related weather at this stage." After partitioning (and the exclusion of overland cases), 11 cases of weakening and 6 cases of strengthening were found. In similar fashion to this paper, Hart et al. (2006) go on to describe synoptic structures associated with both the intensifying and weakening groups, more specifically the orientation of the tilt of the 500-hPa midlatitude trough and its distance from the polewardmoving tropical cyclone. Meanwhile, Ritchie and Elsberry (2007) use model simulations of both intensifying and dissipating cases to investigate the impact of the midlatitude trough with respect to its intensity, orientation, and distance from the tropical cyclone. In addition, Ritchie and Elsberry (2007) investigate the issue of precipitation distributions in their model simulations, for both the intensifying and dissipating cases. It is first and foremost believed that because of the relatively small sample sizes in Hart et al. (2006), Ritchie and Elsberry (2007), and this paper, that certain results prevalent in all three papers should be taken as a reinforcement of those particular results. A more specific and in-depth discussion of the results of both Hart et al. (2006) and Ritchie and Elsberry (2007) and the importance of these results to those reported in this paper can be found in section 3.

Most of the research with respect to eastern Canada examines the transition and subsequent reintensifications of Hurricanes Earl (in 1998; McTaggart-Cowan et al. 2003, 2004a; Ma et al. 2003; McTaggart-Cowan et al. 2004a; Elsberry 2004; McTaggart-Cowan et al. 2004b) and Michael (in 2000; Fogarty 2002a; Abraham et al. 2002). While Fogarty and Gyakum (2005) and Gyakum (2003) produce dynamic analyses of ET in eastern Canada through 1996, no study objectively analyzes the precipitation distributions associated with transitioning cyclones in eastern Canada in similar fashion to what Atallah et al. (2007) does for the United States. This is despite the significant number of flooding events resulting from northward-moving tropical cyclones affecting eastern Canada over the last three decades.

To this end, Atallah et al. (2007), Jones et al. (2003), and DiMego and Bosart (1982a), among others, cite the impact of ET in terms of catastrophic flooding potential. Quite a few of these storms from Agnes (in 1972; DiMego and Bosart 1982a,b) to Katrina (2005) are responsible for copious amounts of precipitation even after ceasing to be tropical cyclones. Atallah et al. (2007) seek an evaluation of precipitation distributions associated with landfalling, and subsequently northward-moving, remnants of tropical cyclones. Meanwhile, Darr (2002) chooses a set of tropical cyclones in the western North Atlantic basin and classifies them as storms that underwent either a strong transition or no transition at all during their life cycle.

McTaggart-Cowan et al. (2004b) state: "As both a forecasting and a diagnostic tool, it is often convenient to sort features involved in the ET process into the mutually exclusive categories of either tropical or extratropical. Such a simplification is useful to the extent

that it allows us to define a common framework under which to discuss these events; however, it can lead to an incorrect conclusion that these features exist in isolation of each other and of their life cycles.'' Accordingly, it is not a priority of this study to define the exact phase each storm is in during the period of study. This is a major contrast of this paper with the work of Hart et al. (2006) and Ritchie and Elsberry (2007). It is important to explicitly state, therefore, that it is not an a priori constraint that the cases in this paper have or are undergoing ET; that is, the transition of a purely tropical cyclone to one with purely extratropical or hybrid characteristics (Jones et al. 2003). However, it is certainly reasonable, based on past research (mainly Hart and Evans 2001) and general meteorological knowledge, to assume that many of the cases in this study do involve ET simply because of the relatively high latitudes in eastern Canada where most of the cases are studied. This subtle but important distinction will be expanded upon later in this paper, primarily in section 3a.

Finally, it is often convenient in synoptic meteorology to ignore diabatic and frictional effects, so as to make equations and diagnostics easier to use. In terms of the storms in this study, however, an interaction takes place that is essentially the ''juxtaposition of two very different air masses (tropical and baroclinic) resulting in a pronounced temperature gradient. . .that can lead to copious amounts of precipitation. The diabatic heating resulting from the precipitation then serves as a mechanism for changing the scales and orientations of the upper and lower-level potential vorticity (PV) anomalies'' (Atallah and Bosart 2003). Atallah and Bosart (2003) also find that, in the case of Hurricane Floyd (1999), diabatic heating released by heavy precipitation along the U.S. east coast acted to enhance the downstream ridge over the western Atlantic; this subsequently changes the orientation of the midlatitude trough interacting with Floyd from positive (i.e., a trough axis from southwest to northeast) to negative (i.e., a trough axis from southeast to northwest), making it more potent. Colle (2003) agrees, stating that high-resolution modeling of Floyd clearly shows that, when diabatic effects are removed, the storm is approximately 25 hPa weaker at sea level than when diabatic effects are included. It is evident from the literature that diabatic heating is an important aspect of poleward-moving tropical cyclones, since it can affect the storm in multiple ways, from intensity and track of the cyclone, to copious amounts of precipitation. Therefore, the importance of diabatic processes will be highlighted as one that is quite nonnegligible, particularly in cases of rapid reintensification of tropical and ex-tropical cyclones in the midlatitudes.

b. Objectives

One goal in this study is to combine the dynamical approach of Darr (2002) and the precipitation focus of Atallah and Bosart (2003) and Atallah et al. (2007), while utilizing a much higher-resolution dataset [the National Centers for Environmental Prediction (NCEP) North American Regional Reanalysis (NARR; Mesinger et al. 2006)], to help resolve features not previously examined using lower-resolution analyses. Specifically, it is important to contrast two methodologies: (i) using precipitation distributions to perform a dynamical analysis (as in Atallah et al. 2007) and (ii) using dynamical storm partitioning to analyze precipitation distributions (as done in this study).

In summary, the main objectives of this paper are as follows:

- Partition the storm cases into ''intensifying'' and ''decaying'' groups, based on an intensity criterion (section 3a).
- Explore the similarities and differences between the intensifying and decaying groups by examining various synoptic structures, using both quasigeostrophic (QG) and PV thinking (section 3b).
- Compare and contrast the precipitation distributions of the storms in the intensifying and decaying groups (section 3c).
- Investigate effects of latent heat release due to intense precipitation on synoptic structures, for both the intensifying and decaying groups (section 3d).

2. Data

Storm cases are chosen from the National Hurricane Center (NHC) best-track archive dataset (see online at http://www.nhc.noaa.gov). In total, 40 storms are found to have tracked over eastern Canada (from Windsor, Ontario, to St. John's, Newfoundland) from 1979 to 2005 (Fig. 1), as listed in Table 1.

Both the NCEP–National Center for Atmospheric Research (NCAR) global reanalysis (Kalnay et al. 1996) and the NCEP NARR (Mesinger et al. 2006) are utilized in this study. However, the NARR, which has a 32-km horizontal resolution (as opposed to a 2.5° horizontal grid in the global reanalysis), higher temporal resolution (3 versus 6 h), and the availability of a 3-hourly accumulated precipitation field, is chosen as the primary dataset for analysis. The primary use of the NCEP global reanalysis is to plot composites. Unlike the NCEP global reanalysis, which encompasses data back to 1948, the NARR data begins in 1979. As a result, the storm dataset for this study is limited to 1979–present. It is worth noting before proceeding that the NARR has

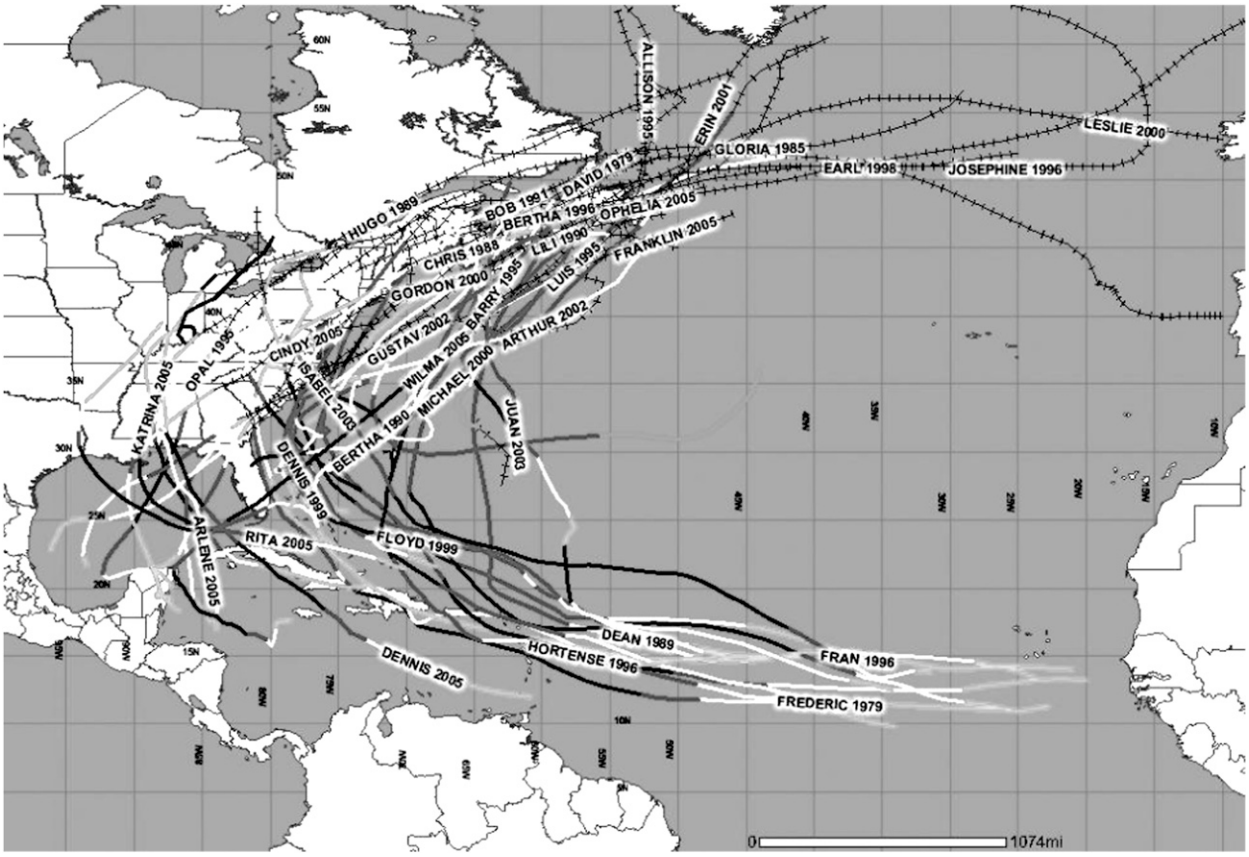

FIG. 1. All 40 storm cases, as represented by their individual storm track (1979–2005). Solid lines indicate that the NHC best-track data reports the storm as tropical (with different shades of gray representing various intensities, which is irrelevant to this paper), while lines with ticks represent storms after they have undergone ET, as determined by the NHC.

documented limitations, especially with respect to its handling of warm-core tropical cyclone–like vortex structures, despite having a higher resolution than other global reanalyses. While this is not a huge concern for this paper given that the NARR is used mostly for precipitation distribution analysis and that most of the storms in this study are at high enough latitudes such that the storm is no longer tropical, the authors would prefer the reader to be aware of the limitations of the NARR. In addition, it is of note that the NARR 3-hourly precipitation field is composed of model precipitation data over the ocean and observation-based data over the continental United States. In Canada, the precipitation over land is observation based through 2002 and model based after that (M. Carrera 2005, personal communication). Mesinger et al. (2006) state that while the NARR precipitation is not perfect, ''the assimilation of precipitation during the reanalysis was found to be very successful, obtaining model precipitation quite similar to the analyzed precipitation input.'' Therefore, one can conclude that even when using model-based precipitation, the NARR does as good as job as any available dataset. Moreover, it is important to keep in mind that for the purpose of this paper, we are interested in the qualitative representation of the precipitation distributions, and not exact precipitation amounts over a given region.

Finally, most of the calculations and analyses in this study are performed and displayed using the General Meteorological Package, version 5.7.4 (Koch et al. 1983).

3. Results

a. Dynamical partitioning

The primary objective of large-scale composite synoptic analyses is to examine the similarities and differences in synoptic structure between intensifying and decaying storms. Thus, the goal of the partitioning methodology is to differentiate between intensifying and decaying storms, based on the rates of change of the layer-averaged low-level vorticity (850–700 hPa), as defined by the quasigeostrophic vorticity equation (Bluestein 1992),

TABLE 1. Storms that are intensifying, decaying, or neither, as listed by year.

Yr	Intensifying	Decaying	Neither
1979	None	David and Frederic	None
1985	Gloria	None	None
1989	None	Hugo	Dean
1990	Bertha	None	Lili
1991	None	Bob	None
1995	Allison, Barry, and Luis	Opal	None
1996	None	Bertha, Fran, and Hortense	Josephine
1998	Earl	None	None
1999	None	Floyd	None
2000	Leslie, Michael	Gordon	None
2001	Erin	None	Karen
2002	Arthur, Gustav	None	None
2003	None	Isabel	Juan
2004	None	None	Frances
2005	Cindy, Katrina, Ophelia, Rita, and Wilma	Dennis	Arlene and Franklin

where η is the geostrophic absolute vorticity (s^{-1}), f_0 is the Coriolis parameter (s^{-1}), and δ is divergence (s^{-1}):

$$\frac{D\eta}{Dt} = -f_0\delta. \quad (1)$$

The four weakest vortices in the study [Alberto (1988), Chris (1988), Unnamed (1991), and Dennis (1999)] have minimum central pressure values more than one standard deviation above the average minimum central pressure; therefore, these storms are dropped from the composite study. This is done so that a very weak system will not be classified in the intensifying category, even if the system does undergo a slight intensification. The remaining 36 storms are partitioned into two groups: intensifying and decaying, based on the rate of change of the depth-averaged low-level (850–700 hPa) absolute vorticity. An intensifying case is chosen to be defined by a minimum low-level absolute vorticity increase of $5 \times 10^{-5}\,s^{-1}$ over a time period of 12 h, while a decaying case is chosen to be defined by a decreasing absolute vorticity of similar magnitude. While the above intensity criterion is believed to be used for the first time in this study, it is believed that this value is even more stringent than the 4 hPa of minimum sea level pressure every 24 h utilized in Hart et al. (2006). For example, Fig. 2 displays the strongly positive slopes (vorticity increases) at both the mid- (700–400 hPa) and low (850–700 hPa) levels for the most rapidly intensifying case in the study: Luis (1995). In contrast, Fig. 3 displays strongly negative slopes (vorticity decreases) at both the mid- and low levels for the most rapidly decaying case in the study, Isabel (2003). We find that 16 storms fit the intensifying criterion, while 12 cases are categorized as decaying (Table 1). The remaining eight storms did not exhibit a large enough low-level vorticity tendency to meet the partitioning criteria in either direction.

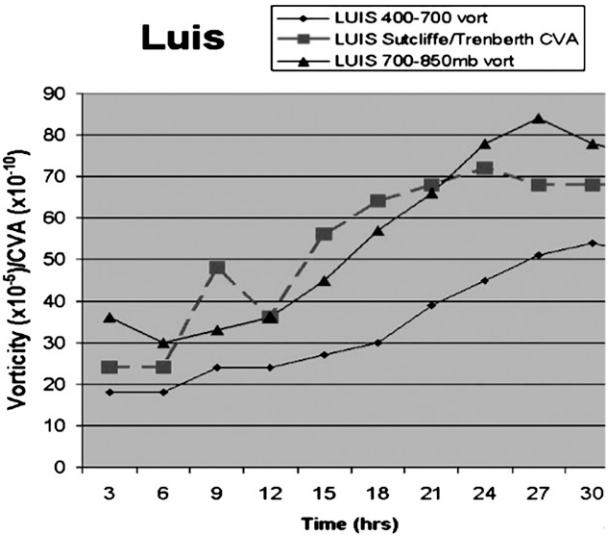

FIG. 2. For Luis (1995): NARR 700–400-hPa absolute vorticity ($\times 10^{-5}\,s^{-1}$, solid with dots), 850–700 absolute vorticity ($\times 10^{-5}\,s^{-1}$, solid with triangles), cyclonic vorticity advection (CVA) from Eq. (2), by the Trenberth method ($\times 10^{-10}\,s^{-2}$, dashed with squares); $t = 0$ represents the time the storm is judged to have begun to affect Canada.

Now that the criterion for intensifying and decaying storms has been defined, it is important at this juncture to support the statements made in section 1b regarding

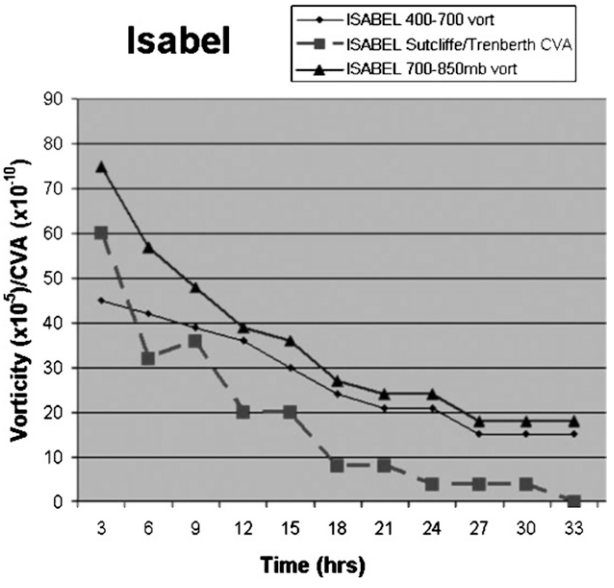

FIG. 3. As in Fig. 2, but for Isabel (2003).

why we largely ignore whether the cases in this paper are undergoing or have undergone ET. Again, while it is probable that most of the cases in this study are storms that are undergoing or have undergone ET, the main objectives of this paper are the synoptic structures and the precipitation distributions of the intensifying and decaying composite groups. That is, it is more important, for the scope of this paper, to focus on the intensification–decay criterion than on whether a storm has undergone ET. This is primarily due to the ambiguity that (particularly in the decaying composite) there are cases of storms that do undergo ET and storms that remain purely tropical into the region of study.

b. Composite synoptic structures

It is important that when investigating the synoptic structures of the two composite groups (intensifying and decaying) that both QG and PV perspectives are utilized. It is crucial to note that in this paper, when referencing QG thinking, perspectives and plots, we are referring to the Trenberth approximation to the quasigeostrophic omega equation, which is given and described in section 3b(1). This approximation excludes diabatic and frictional effects.

While it is true that many of the structures observed in the QG plots (Fig. 4) can also be seen in the PV plots (Fig. 5), a view of the total QG forcing for ascent (Fig. 4) allows us to observe the midlatitude dynamics responsible for the forcing of upward vertical motion (and thus precipitation), without any explicit diabatic effects. While PV thinking may allow for a more complete view of all synoptic-scale processes, the Trenberth formulation (or QG view) allows for the isolation of the nondiabatic processes.

All composite plots are produced using a storm-relative compositing method (Atallah et al. 2007). This process involves compositing the storm cases relative to a specific latitude–longitude point based on a reference storm track. In this study, the reference storm track chosen for each group is an average position of the cases in the group. For example, all the grids in the intensifying composite at time $t = 0$ are shifted so that each storm center is located at the same latitude–longitude coordinate, as specified by the reference storm track. Therefore, all motion of the composite storm is relative to the reference track and not to the apparent geography on the map. The geography is retained on the plots, however, for the purposes of scale, discussion of relevant features, and as a reminder that the study is based in the western North Atlantic basin. Storm positions at each time are generally within 5° latitude of each other, therefore minimizing curvature (with respect to the earth) problems (Atallah et al. 2007).

1) QUASIGEOSTROPHIC PERSPECTIVE

This study follows the method of Atallah and Bosart (2003) and depicts 1000–200-hPa thickness values with 700–400-hPa layer-averaged absolute vorticity. Absolute vorticity and relative vorticity are qualitatively interchangeable in the midlatitudes within the Trenberth approximation (Trenberth 1978) to the quasigeostrophic omega equation [Eq. (2)], since the advection of planetary vorticity can be ignored where the thermal wind shear tends to be westerly and the Coriolis parameter varies only meridionally (Bluestein 1992). The Trenberth approximation [Eq. (5.7.42) on p. 349 of Bluestein (1992)], where f_0 is the Coriolis parameter (s^{-1}), σ is the static stability parameter ($m^2\ s^{-2}\ kPa^{-2}$), ω is the vertical velocity in pressure coordinates (hPa s^{-1}), $\mathbf{v}_g$ is the geostrophic wind vector (m s^{-1}), and $\nabla_p\zeta_g$ is the gradient of geostrophic relative vorticity on a constant pressure surface ($m^{-1}s^{-1}$), is as follows:

$$\left(\nabla^2 p + \frac{f_0^2}{\sigma}\frac{\partial^2}{\partial p^2}\right)\omega = \frac{f_0}{\sigma}2\left(\frac{\partial \mathbf{v}_g}{\partial p}\cdot\nabla_p\zeta_g\right). \qquad (2)$$

Areas of large values of cyclonic vorticity advection by the thermal wind coincide with large values of synoptic-scale forcing for ascent, as dictated by Eq. (2). Thus, one can stipulate that in an intensifying storm in which the vorticity is increasing over time [Eq. (1)], the values of cyclonic vorticity advection will increase over a given baroclinic zone, thus likely increasing the upward vertical motion and resulting precipitation [Eq. (2)].

Composite images are displayed for $t = -12$ h, $t = 0$ h, and $t = 12$ h, where $t = 0$ h is defined as the initial time that the low-level absolute vorticity begins to change, as defined in the compositing methodology. Important similarities and differences in the dynamical structures of the intensifying and decaying composites include the following:

- At $t = -12$ h, the precursor trough seen on the map near the Great Lakes in intensifying cases (Fig. 4a) is more dynamically active than the trough found in the decaying composite (Fig. 4d). This conclusion is drawn from both the negative tilt of the aforementioned trough and the shorter trough–ridge wavelength seen in the intensifying cases over the mid-Atlantic states.
- The tilt of the precursor trough and its geographical proximity to the tropical cyclone are crucial. In particular, the trough has a noticeable negative tilt in the intensifying composite (Figs. 4a,b), as well as being physically closer to the tropical cyclone than in the decaying cases (Figs. 4d,e). This suggests that the ''tilt'' and proximity of the trough to the cyclone are just as

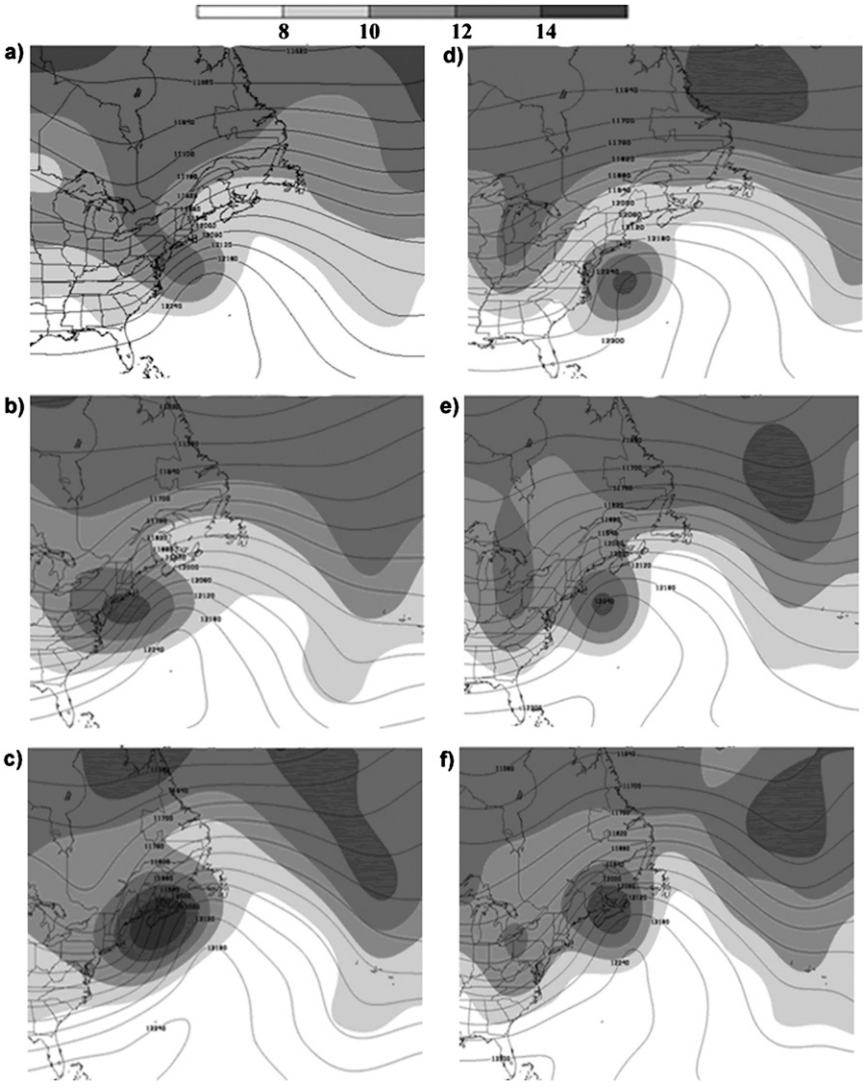

FIG. 4. (a) Intensifying QG grid-centered composite at $t = -12$ h, with 700–400-hPa layer-averaged relative vorticity ($\times 10^{-5}$ s^{-1}, shaded) and 1000–200-hPa thickness (m, contoured). (b) As in (a), but for $t = 0$ h. (c) As in (a), but for $t = +12$ h. (d) Decaying QG grid-centered composite at $t = -12$ h, with 700–400-hPa layer-averaged relative vorticity ($\times 10^{-5}$ s^{-1}, shaded) and 1000–200-hPa thickness (m, contoured). (e) As in (d), but for $t = 0$ h. (f) As in (d), but for $t = +12$ h.

important as the intensity. These findings are in agreement with Hart et al. (2006), who despite using a different intensification criterion, found similar synoptic structures for both the intensifying and decaying cases. In fact, Hart et al. (2006) explicitly state that ''the separation distance between the trough and TC varies considerably between the composites, with the post-ET intensifier having a much closer approach than the post-ET weakener.'' Moreover, Hart et al. (2006) performed a time sequence of Eliassen–Palm flux divergence for both their intensifying and weakening composites and found that in the intensifying composite, ''the negative trough tilt both permits the TC to approach the trough to a much smaller distance, and also drives heat and momentum fluxes that amplify the trough itself…'' This is a crucial finding given the similarities in synoptic structures between the Hart et al. (2006) results and those found in this paper for both composite groups. Finally, the agreement between the two studies is also interesting given that in this paper, there is no explicit a priori assumptions about ET, while in Hart et al. (2006), ''intensification'' and ''decay'' are assumed to be ''post-ET.''

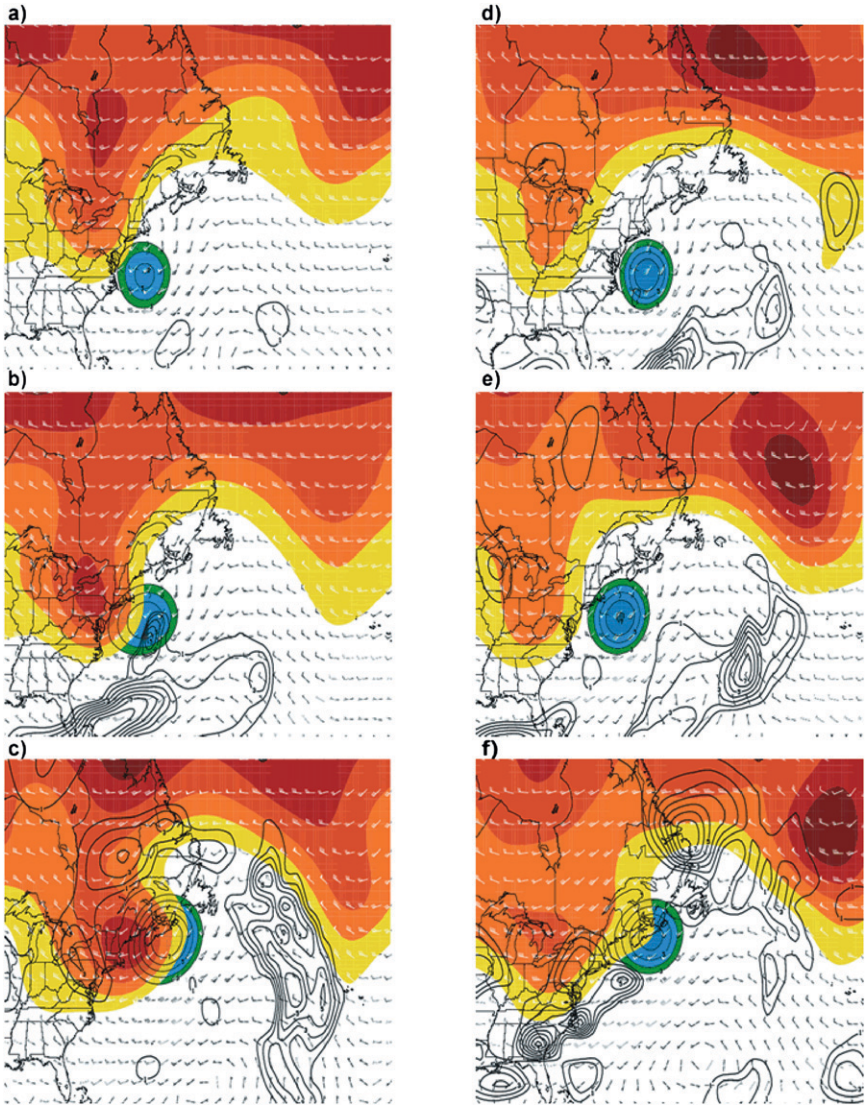

FIG. 5. (a) Intensifying PV composite at $t = -12$ h, with 300–200-hPa PV shaded every 1 PVU (warm colors), 850–700-hPa relative vorticity shaded and contoured every 2×10^5 s^{-1} (cool colors), 850-hPa (300 hPa) winds overlayed in black (white), and 6-h change due to diabatic heating of potential temperature on the dynamic tropopause in solid black contours, every 1 K. (b) As in (a), but for $t = 0$ h. (c) As in (a), but for $t = +12$ h. (d) As in (a), but for the decaying composite at $t = -12$ h. (e) As in (d), but for $t = 0$ h. (f) As in (d), but for $t = +12$ h.

- The increase in scale of the tropical cyclone at $t = +12$ h is more significant in the intensifying composite (Fig. 4c) than in the decaying storms (Fig. 4f).
- The downstream ridge is more amplified in the intensifying cases (Figs. 4b,c) following the interaction of the upstream trough and the tropical cyclone, in the region of northeastern Canada. This process occurs as a cycle, where the tropical cyclone interacts with the midlatitude trough, thereby reintensifying the surface cyclone, causing heavier precipitation, which through latent heat release builds the ridge on the cyclone's northern flank, which in turn collapses the trough–ridge wavelength and allows the surface cyclone to intensify further because of increased cyclonic vorticity advection over it, in association with the collapsed wavelength. This process is further discussed in section 4.

2) POTENTIAL VORTICITY PERSPECTIVE

Potential vorticity composites are very useful in ET studies because of the conservative property of PV in an adiabatic frictionless environment (Hoskins et al. 1985;

Morgan and Nielsen-Gammon 1998). In other words, areas of intense diabatic heating due to latent heat release from heavy precipitation are easily identifiable on a PV map, represented as areas of nonconservative PV. In addition, the PV composites in the study allow observation of the interaction between the low-level (tropical) and midlevel (trough) systems on one map (Atallah et al. 2007). To observe interactions between upper-tropospheric and lower-tropospheric features, all PV composite maps composed of 300–200-hPa PV (warm colors) and 850–700-hPa relative vorticity (cool colors) with winds at both the upper (white) and lower (black) levels overlaid. High values of PV at a near-tropopause level (300–200 hPa) represent cyclonic (trough) features, while low values of PV suggest an anticyclonic (ridge) feature. In addition, 6-h changes in the total derivative of the potential temperature on the dynamic tropopause are used to assess diabatic processes only, and are contoured in solid black and are discussed below in section 3d. This change in potential temperature on the dynamic tropopause is computed by subtracting the local change and change due to advection only from the total change over 6 h, as seen in Eq. (3), where θ is the potential temperature on the dynamic tropopause and **v** is the wind vector:

$$\frac{D\theta}{Dt} = \frac{\partial\theta}{\partial t} + \mathbf{v} \cdot \nabla\theta. \tag{3}$$

Important conclusions about dynamic structures in the PV composites include the following:

- As seen in the quasigeostrophic composites, the upstream trough is more dynamically active (i.e., has more of a negative tilt) and closer to the tropical cyclone in the intensifying composite (Fig. 5a) than in the decaying composite (Fig. 5d) at $t = -12$ h.
- Prior to interaction with midlatitude features (at $t = -12$ h), the tropical cyclone has higher values of lower-tropospheric relative vorticity in the decaying composite (Fig. 5d) than in the intensifying composite (Fig. 5a). This result in the decaying composite suggests that the storm retains its purely tropical characteristics as it remains underneath a large-scale ridge environment. Moreover, the close proximity of the upper-level trough to the tropical cyclone in the intensifying composite has caused the storm to weaken due to the presence of wind shear, whereas the upper-level trough and tropical cyclone are located far enough apart that this does not occur in the decaying composite. However, in the decaying composite, as the tropical cyclone becomes extratropical, its position underneath the large-scale ridge is no longer favorable for intensification (i.e., the proper dynamics are not in place to prevent the storm from weakening rapidly due to shear effects).
- At $t = 12$ h, the intensifying composite (Fig. 5c) shows a marked increase in scale and intensity of the formerly tropical cyclone, following 12 h of sustained interaction and coupling with the midlatitude trough. The decaying composite (Fig. 5f) does not depict any such scale increase. The observation of a marked increase in scale and intensity of the cyclone is to be viewed with a caveat that the cyclone is entering a region of more observations (i.e., the midlatitudes); while the effect of this cannot be quantified, it is worth being aware of.
- The downstream ridge becomes progressively more amplified from $t = -12$ h to $t = +12$ h in the intensifying cases, unlike in the decaying composite. At $t = +12$ h, the intensifying composite (Fig. 5c) shows an impingement of the ridge on the upstream trough to the northwest of the transitioning cyclone. The enhancement of the ridge, depicted by positive values (black contours) of the total change of the derivative of potential temperature on the dynamic tropopause [Eq. (3)], is possibly due to latent heat release from heavy precipitation associated with the intensifying system. No similar westward ridge impingement is seen in the decaying composite (Fig. 5f). This observation is consistent with the counterclockwise rotation of precipitation in the intensifying composite, depicted in the following section, and is further discussed in section 3d.

c. *Precipitation distribution*

Precipitation distributions are important consequences of and factors in the dynamics of a storm undergoing ET. For many of the intensifying cases, the NARR 3-hourly accumulated precipitation field shows evidence of a counterclockwise rotation around the cyclone as it transitions and explosively reintensifies at high latitudes. In contrast, many of the decaying cases exhibit an anticyclonic rotation around the low pressure center during storm weakening. These results are consistent (particularly in the intensifying composite) with those found in the simulations completed by Ritchie and Elsberry (2007), who found that in the intensifying cases the precipitation distributed went from being collocated with the tropical cyclone center to the northeast and finally northwests quadrant of the reintensifying extratropical cyclone.

Figure 6 illustrates precipitation distributions of the 16 intensifying storms prior to intensification. Note that prior to intensification, the majority of the precipitation is to the east or northeast of the surface low pressure

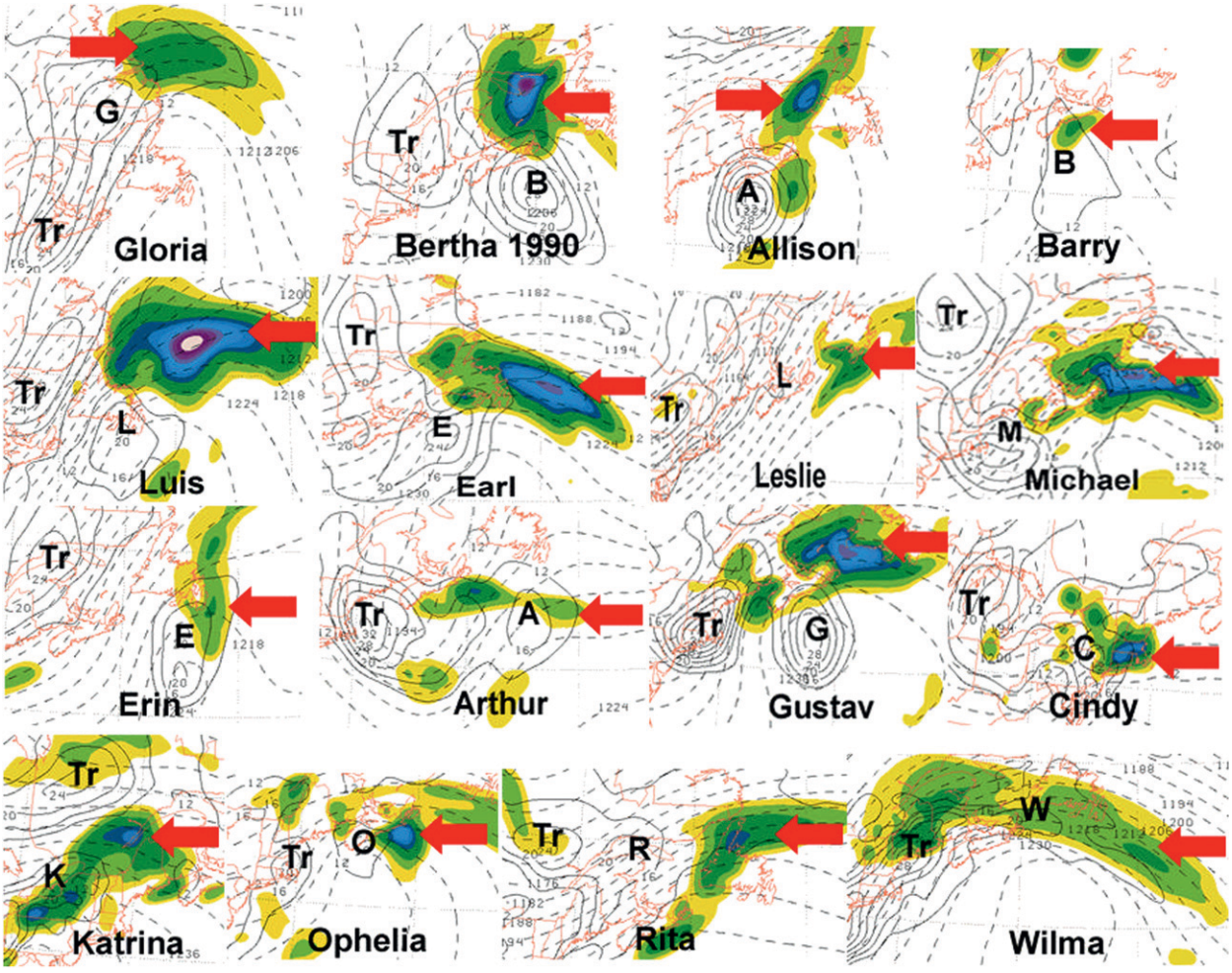

FIG. 6. The 16 intensifying storms and their precipitation distributions just prior to explosive intensification; NARR 3-hourly precipitation (every 2 mm, shaded), NARR 700–400-hPa absolute vorticity ($\times 10^{-5}$ s^{-1}, solid contours), NARR 1000–200-hPa thickness contours (m, dashed contours).

center (labeled by the first letter of the storm's original name), with the exception of Bertha (1990), in which the main area of rainfall is located to the north of the surface low center. Consequently, Fig. 7 shows that at a time 12–24 h later, the main regions of precipitation have rotated cyclonically around the surface's low pressure center, following the interaction of the storm with the upstream upper-level trough. Thus, the location of the main area of rainfall during and after explosive reintensification tends to be in the northwestern quadrant, particularly for the more rapidly deepening cases, such as Luis (1995) and Earl (1998). These findings support the assertion of DiMego and Bosart (1982a), who state that as the storm intensifies, regions of lower-tropospheric warm air advection (WAA) and intense diabatic heating (and thus, the regions of precipitation) rotate cyclonically around the storm. The results found for the intensifying cases are in direct contrast with those found in the decaying cases. As seen in Fig. 8, the precipitation structures are inconsistent among the 12 cases prior to storm decay. However, consistency becomes evident in Fig. 9, where 12–24 h after decay begins, many of the cases in this composite see an anticyclonic rotation of the main precipitation area around the surface's low pressure center. Furthermore, the areal extent of the precipitation region gets smaller over time, as do accumulated precipitation amounts. In general, the region of precipitation is located to the east of the storm following cyclone decay. This precipitation is most likely still in the region of strongest warm air advection, albeit as the storm weakens, the region of strongest warm air advection is located farther away from the surface's low pressure center, evidenced by the larger distance between the main precipitation

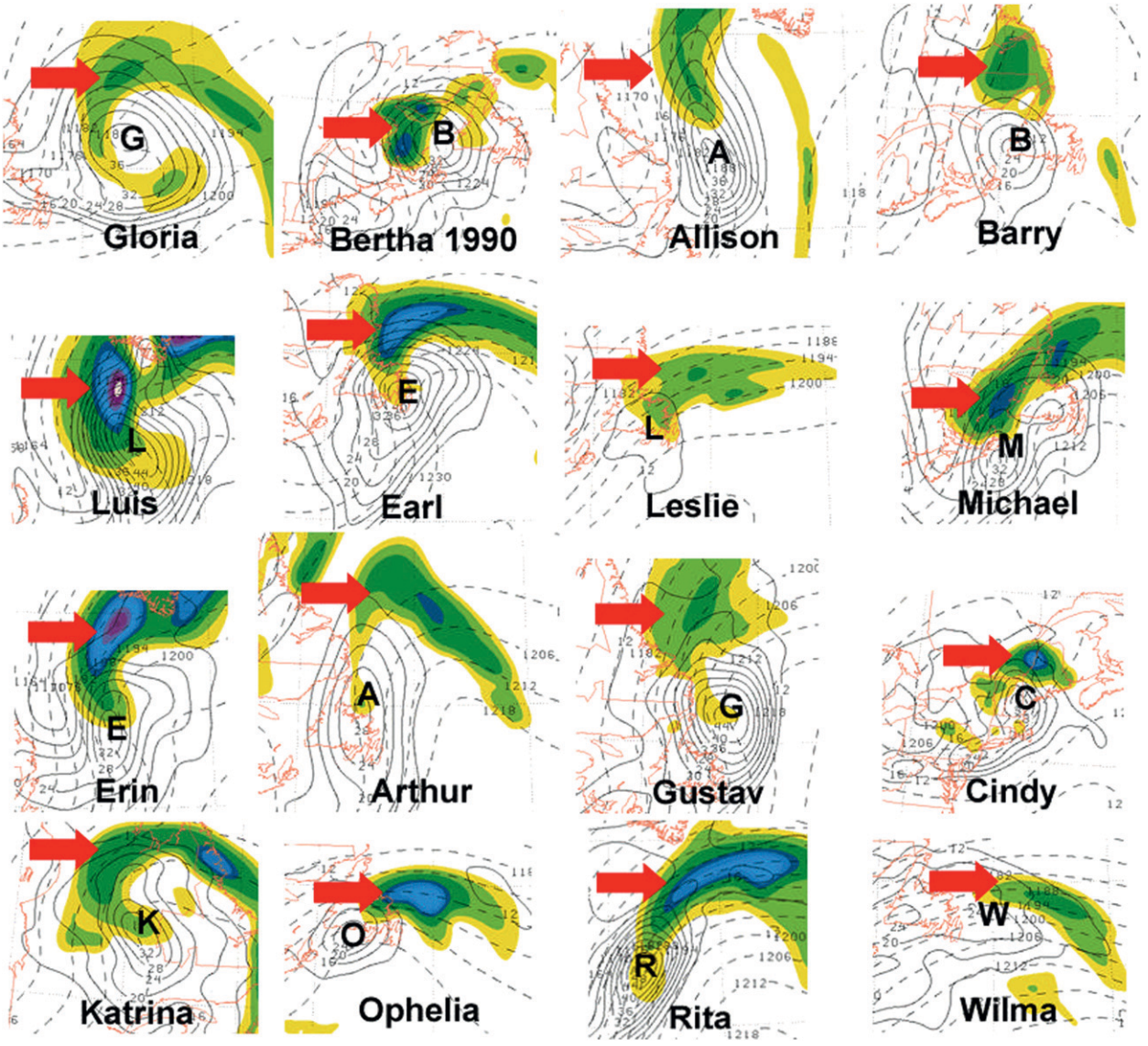

FIG. 7. The 16 intensifying storms and their precipitation distributions just after explosive intensification; parameters are the same as in Fig. 6.

area and the low pressure center in many of the decaying cases.

d. Diabatic heating

A positive feedback on the synoptic-scale environment associated with diabatic heating, if present, consists of three steps: 1) latent heat release from heavy precipitation associated with the cyclone, 2) PV redistribution from latent heat release acts to enhance the downstream ridge, and 3) the enhancement of the downstream ridge results in a collapse of the wavelength between the trough and ridge, leading to a negative tilted trough and increased differential cyclonic vorticity advection directly over the surface cyclone center:

$$V\frac{\partial\theta_b}{\partial s} < 0. \tag{4}$$

It has already been demonstrated that in rapidly reintensifying cases of ET, the precipitation distribution rotates cyclonically around the low pressure center over time. Accordingly, the most intense area of diabatic heating due to latent heat release from heavy precipitation should also be expected to rotate in a similar fashion. Figure 5 shows this by displaying the 6-h positive change in potential temperature due to diabatic heating only (in solid black contours). In addition, Figs. 10a–c and 11a–c examine this feature by displaying the 200-hPa anticyclonic curvature, which is defined in Eq. (4), where V is

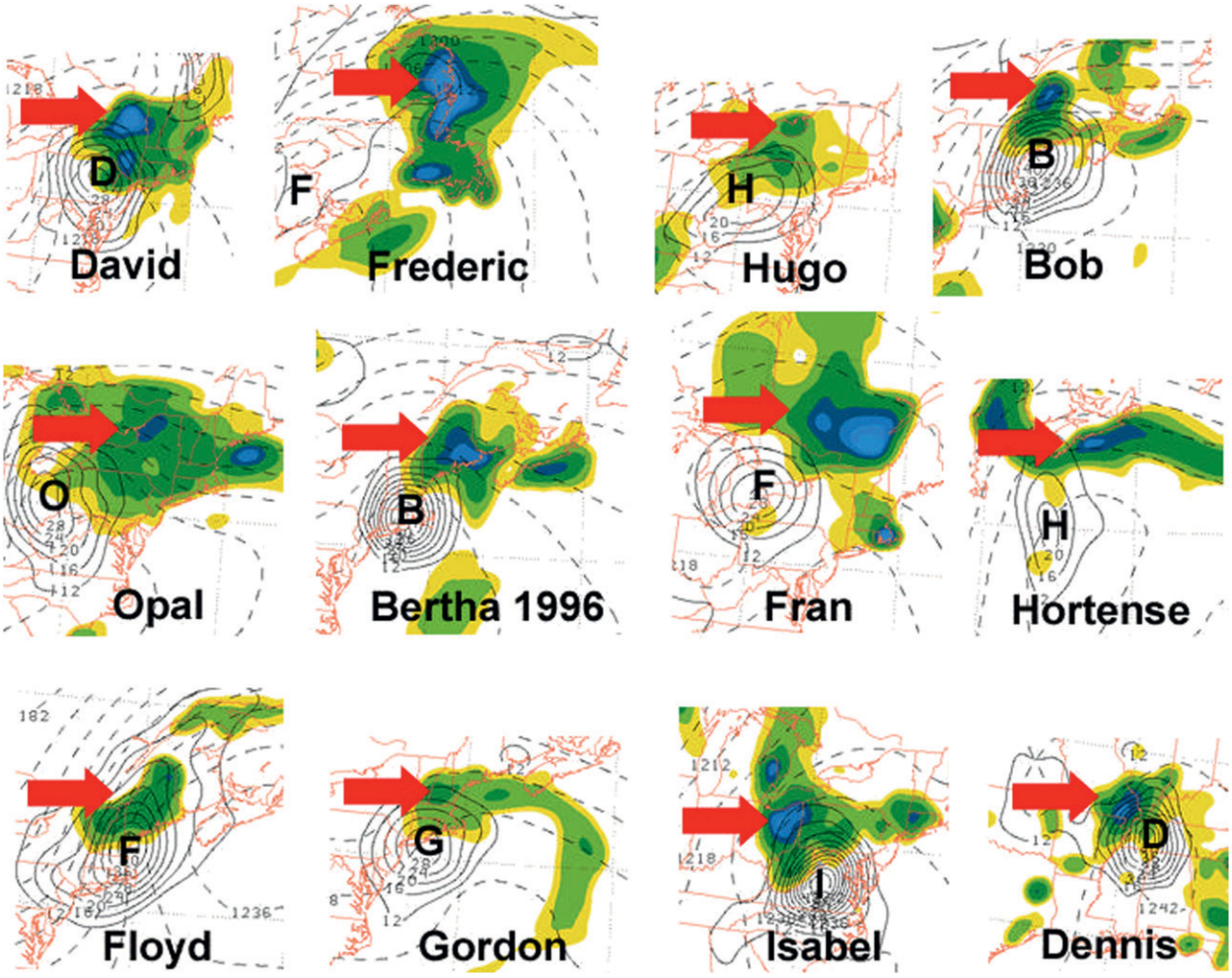

FIG. 8. The 12 decaying storms and their precipitation distributions just prior to decay; parameters are the same as in Fig. 6.

the wind speed, θ_b is the mathematical wind direction, and s represents the x axis in the direction of the wind.

At $t = +12$ h (Figs. 5c,f), one can observe the differences in the 6-h change in potential temperature on the dynamic tropopause on the reintensifying cyclone's immediate northern flank. In the intensifying composite (Fig. 5c), positive values of the abovementioned quantity are located in the region (over Labrador and extreme northeastern Quebec) of the building downstream ridge on the north and northwest side of the reintensifying cyclone. These positive values of potential temperature change due to diabatic heating indicate that latent heat release from heavy precipitation on the cyclone's northern and northwestern flank (shown in section 3c to be the location of the precipitation at $t = +12$ h for intensifying storms) is contributing to the suspected diabatic enhancement of the downstream ridge, which, as explained earlier, then acts to enhance the reintensifying cyclone by collapsing the wavelength of the trough–ridge couplet and thus increasing the CVA over the surface cyclone center. A similar conclusion cannot be made for the decaying composite (Fig. 5f), where no positive contours of potential temperature change on the dynamic tropopause are observed in the region of the cyclone's immediate northern and northwestern flank. This finding indicates that there is a lack of heavy precipitation (as discussed in section 3c) at $t = +12$ h, which would potentially contribute to the diabatic enhancement of the downstream ridge.

Figures 10a–c display the apparent retrogression of the downstream ridge as the cyclone undergoes rapid intensification from $t = -24$ h (Fig. 10a) to $t = +24$ h (Fig. 10c). On the northern and northwestern flank of the expanding and intensifying cyclone, the downstream ridge impinges upon the upstream trough in an upshear sense over time, suggesting that latent heat release plays

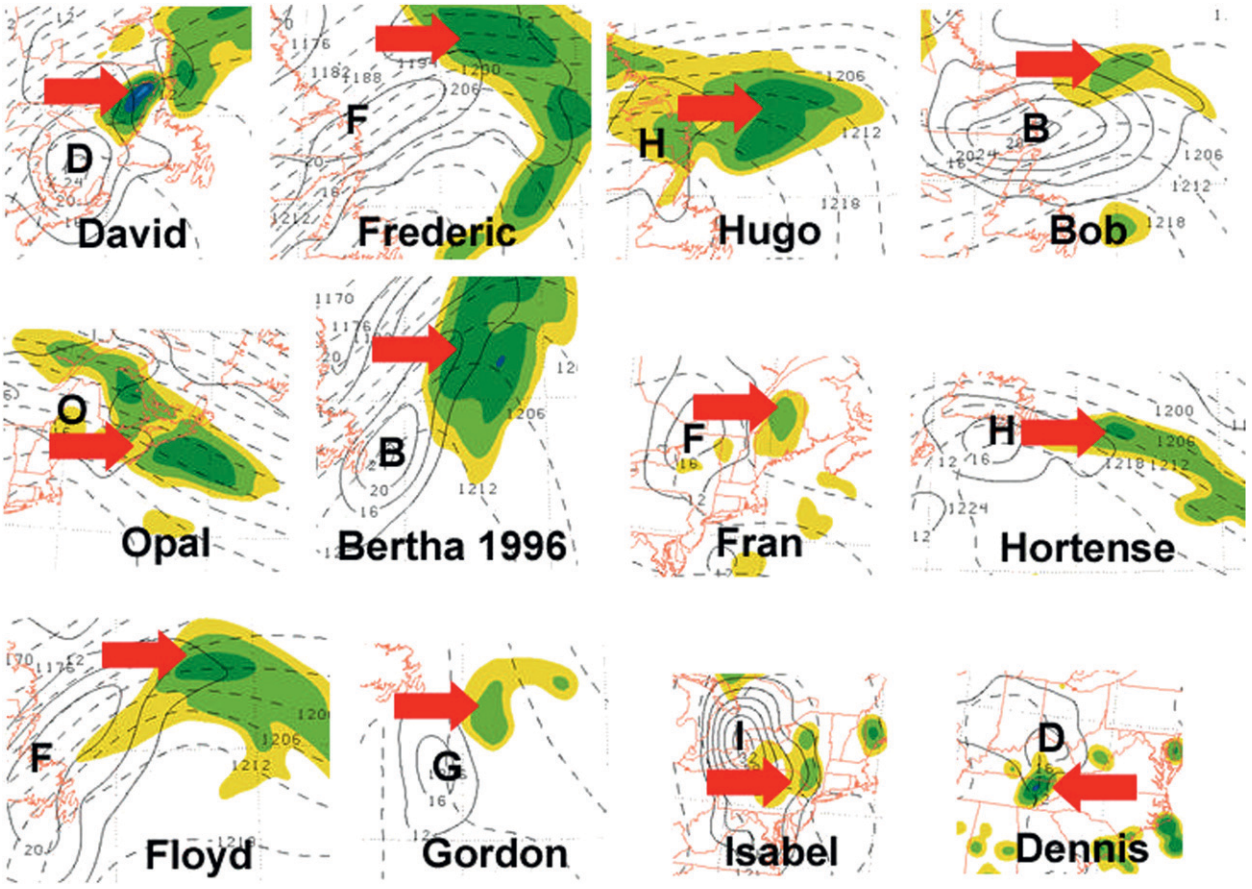

FIG. 9. The 12 decaying storms and their precipitation distributions just after rapid decay; parameters are the same as in Fig. 6.

a prominent role in this process. Moreover, the intensifying cyclone and the downstream ridge appear to propagate as a couplet, with the cyclone remaining near the inflection point in the intensifying composite (Figs. 10a–c), contrary to its clear entry into the ridge environment in the decaying composite (Figs. 11a–c). This suggests that while there is a coupling of the two features in the intensifying composite (Fig. 10) primarily

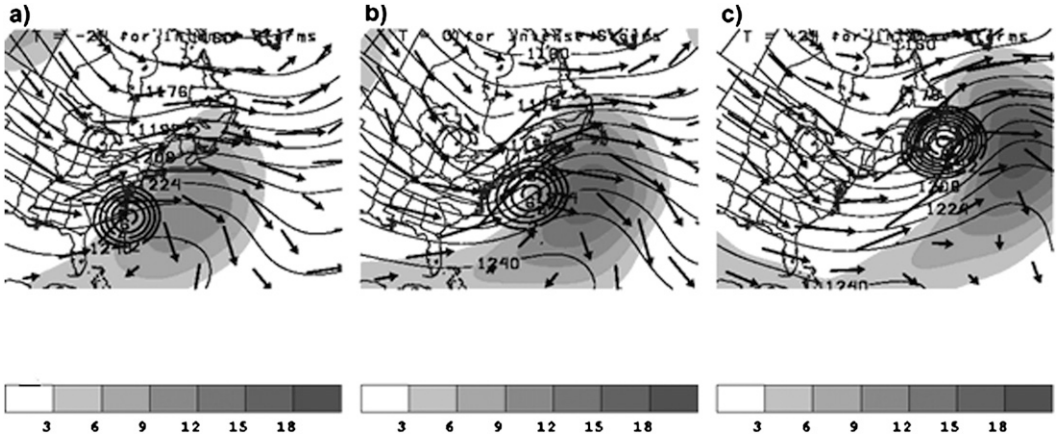

FIG. 10. Intensifying composite at (a) $t = -24$ h, (b) $t = 0$ h, and (c) $t = +24$ h, with NCEP global reanalysis 850–200-hPa wind shear (arrows), 200-hPa height (light contours), 850-hPa relative vorticity (dark contours), and 200-hPa anticyclonic curvature (shaded).

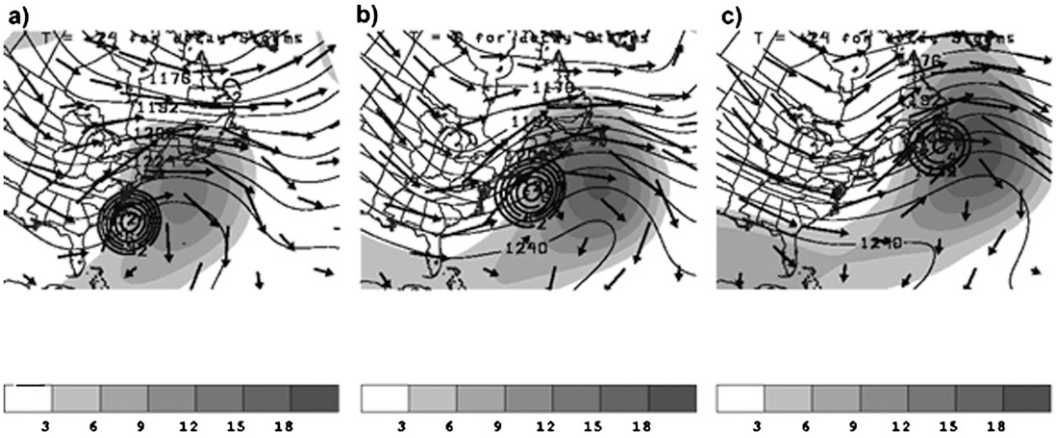

FIG. 11. As in Fig. 10, but for the decaying composite.

due to diabatic processes, there is a lack of such an interaction in the decaying cases. In the decaying composite (Figs. 11a–c), it appears the cyclone is merely advected downshear into an anticyclonic environment from $t = -24$ h (Fig. 11a) to $t = +24$ h (Fig. 11c), which in turn would limit any possible interaction with an upstream midlatitude trough.

4. Conclusions

The extratropical transition of tropical cyclones is an expanding area of research in the atmospheric science community and can have an enormous impact on interests in eastern Canada, because of the potentially damaging winds and catastrophic amounts of rainfall from these cyclones. Little wholly inclusive research has been done on the behavior and effects of these storms in the eastern Canada region. To that end, from 1979 to 2005, 40 cases of transitioning tropical cyclones are selected and dynamically partitioned into intensifying, decaying, and null samples. Subsequently, several important features are analyzed, including composite dynamical structures, precipitation distributions, and frontogenesis.

In total, 16 storms are classified as intensifying, while 12 are classified as decaying; the remaining 12 cases do not fit into either group. It is found that the intensifying and decaying groups have dissimilar synoptic structures that account for the differing responses in reintensification (or lack thereof) in the transitioning cyclone. The importance of scale in an ET reintensification is cited by Atallah and Bosart (2003) and Bosart and Lackmann (1995) and is seen in comparing the intensifying and decaying composites; the increase in size of the transitioning tropical cyclone from $t = 0$ (Figs. 4b,e) to $t = +12$ (Figs. 4c,f) is greater in the intensifying composite than in the decaying composite. This is primarily due to the interaction of the tropical cyclone with an upstream midlatitude trough, which is horizontally closer to the tropical cyclone at $t = -12$ (Figs. 4a,c) and $t = 0$ (Figs. 4b,e) for the intensifying composite than it is for the decaying class at the same times. The tilt of the precursor midlatitude trough is also a factor, appearing more negative in the intensifying composite (Figs. 4a–c). In the decaying composite (Figs. 4d–f), the tilt of the upstream trough remains essentially constant and neutral throughout the entire time period.

The upstream trough is not the only large-scale feature crucial to the evolution of these systems. It is found that the intensity and change in intensity of the downstream ridging also plays a major role in the evolution of the transitioning cyclone. In the intensifying cases, the reintensifying cyclone and the downstream ridge appear to be coupled, in that the cyclone does not enter the anticyclonic environment during reintensification (Fig. 10). Even though the cyclone does not enter the ridge environment, the ridge still has a large effect on the intensity of the cyclone. As the cyclone reintensifies and latent heat is released from heavy precipitation, the ridge builds upshear (westward) on the cyclone's northern flank. In effect, the cyclone then strengthens because the magnitude of the differential cyclonic vorticity advection over the surface cyclone center increases as the trough–ridge wavelength collapses; this stronger circulation in turn produces larger values of warm air advection and more precipitation (latent heat release), which completes the feedback by building the ridge. None of these processes (i.e., ridge–cyclone coupling, diabatic cyclone intensification, and diabatic ridging) occurs substantially in the decaying cases. The transitioning cyclone is simply advected downstream into the anticyclonic environment (Fig. 11), simultaneously

moving further away from any possible interaction with the upstream trough. Furthermore, there is a lack of westward impingement of the ridge into the trough environment due to diabatic processes.

In the intensifying composite, the primary area of heavy precipitation rotates cyclonically around the reintensifying cyclone as the storm progresses forward in time from $t = 0$ (Figs. 6 and 7). This is a significant threat to the Atlantic provinces, where a cyclonic rotation of the heavy precipitation area can cause major flooding along or just inland of the coast, when the heaviest bands of precipitation would otherwise be located safely offshore. The intensifying composite also depicts a generally more organized and intense swath of rainfall than does the decaying composite. Precipitation in the decaying composite (Figs. 8 and 9) tends to rotate anticyclonically from $t = 0$ forward, but also rapidly decreases in both areal coverage and intensity, highlighting the limited flooding potential of the decaying storms.

Acknowledgments. This research has been supported by grants from the Natural Sciences and Engineering Research Council of Canada and the Canadian Foundation for Climate and Atmospheric Sciences. Many thanks are due to the three anonymous reviewers for their input and suggestions. Special thanks to the National Centers for Environmental Prediction (NCEP) for providing access to the NCEP Global Reanalysis and the North American Regional Reanalysis, in addition to Dr. Marco Carrera of Environment Canada, whose knowledge of the NARR was extremely useful during the course of this study.

REFERENCES

Abraham, J., C. Fogarty, and W. Strapp, 2002: Extratropical transitions of Hurricanes Michael and Karen: Storm reconnaissance with the Canadian Convair 580 aircraft. Preprints, *25th Conf. on Hurricanes and Tropical Meteorology*, San Diego, CA, Amer. Meteor. Soc., 12D.4. [Available online at http://ams.confex.com/ams/pdfpapers/35168.pdf.]

Agusti-Panareda, A., C. Thorncroft, G. Craig, and S. Gray, 2004: The extratropical transition of Hurricane Irene (1999): A potential-vorticity perspective. *Quart. J. Roy. Meteor. Soc.,* **130,** 1047–1074.

Anthes, R., 1990: Advances in the understanding and prediction of cyclone development with limited-area fine-mesh models. *Extratropical Cyclones: The Erik Palmén Memorial Volume*, C.W. Newton and E.O. Halopainen, Eds., Amer. Meteor. Soc., 221–253.

Atallah, E. H., and L. Bosart, 2003: The extratropical transition and precipitation distribution of Hurricane Floyd (1999). *Mon. Wea. Rev.,* **131,** 1063–1081.

——, ——, and A. Aiyyer, 2007: Precipitation distribution associated with landfalling tropical cyclones over the eastern United States. *Mon. Wea. Rev.,* **135,** 2185–2206.

Bluestein, H., 1992: *Synoptic-Dynamic Meteorology in Midlatitudes*. Vol. I. Oxford University Press, 431 pp.

Bosart, L. F., and D. Dean, 1991: The Agnes rainstorm of June 1972: Surface feature evolution culminating in inland storm redevelopment. *Wea. Forecasting,* **6,** 515–536.

——, and G. M. Lackmann, 1995: Postlandfall tropical cyclone reintensification in a weakly baroclinic environment: A case study of Hurricane David (September 1979). *Mon. Wea. Rev.,* **123,** 3268–3291.

Browning, K., G. Vaughan, and P. Panagi, 1998: Analysis of an extropical cyclone after its reintensification as a warm-core extratropical cyclone. *Quart. J. Roy. Meteor. Soc.,* **124,** 2329–2356.

——, A. Thorpe, A. Montani, D. Parsons, M. Griffiths, P. Panagi, and E. Dicks, 2000: Interactions of tropopause depressions with an ex-tropical cyclone and sensitivity of forecasts to analysis errors. *Mon. Wea. Rev.,* **128,** 2734–2755.

Carr, F. H., and L. Bosart, 1978: A diagnostic evaluation of rainfall predicitability for Tropical Storm Agnes, June 1972. *Mon. Wea. Rev.,* **106,** 363–374.

Colle, B., 2003: Numerical simulations of the extratropical transition of Floyd (1999): Structural evolution and responsible mechanisms for the heavy rainfall over the northeast United States. *Mon. Wea. Rev.,* **131,** 2905–2926.

Darr, J., 2002: Quantitative measurements of extratropical transition in the Atlantic basin. Preprints, *25th Conf. on Hurricanes and Tropical Meteorology*, San Diego, CA, Amer. Meteor. Soc., 13D.2. [Available online at http://ams.confex.com/ams/pdfpapers/36228.pdf.]

Dickinson, M., L. Bosart, K. Corbosiero, S. Hopsch, K. Lombardo, M. Novak, B. Smith, and A. Wasula, 2004: The extratropical transitions of eastern Pacific Hurricane Lester (1992) and Atlantic Hurricane Andrew (1992): A comparison. Preprints, *26th Conf. on Hurricanes and Tropical Meteorology*, Miami, FL, Amer. Meteor. Soc., 17D.2. [Available online at http://ams.confex.com/ams/pdfpapers/75685.pdf.]

DiMego, G., and L. Bosart, 1982a: The transformation of Tropical Storm Agnes into an extratropical cyclone. Part I: The observed fields and vertical motion computations. *Mon. Wea. Rev.,* **110,** 385–411.

——, and ——, 1982b: The transformation of Tropical Storm Agnes into an extratropical cyclone. Part II: Moisture, vorticity, and kinetic energy budgets. *Mon. Wea. Rev.,* **110,** 412–433.

Elsberry, R., 2002: Predicting hurricane landfall precipitation: Optimistic and pessimistic views from the symposium on precipitation extremes. *Bull. Amer. Meteor. Soc.,* **83,** 1333–1339.

——, 2004: Comments on ''The influence of the downstream state on extratropical transition: Hurricane Earl (1998) case study'' and ''A study of the extratropical reintensification of former Hurricane Earl using Canadian Meteorological Centre regional analyses and ensemble forecasts.'' *Mon. Wea. Rev.,* **132,** 2511–2513.

Fogarty, C., 2002a: Hurricane Michael, 17–20 October 2000. Part I: Summary report and storm impact on Canada. Meteorological Service of Canada, 39 pp.

——, 2002b: Operational forecasting of extratropical transition. Preprints, *25th Conf. on Hurricanes and Tropical Meteorology*, San Diego, CA, Amer. Meteor. Soc., 12D.1. [Available online at http://ams.confex.com/ams/pdfpapers/33172.pdf.]

——, and J. Gyakum, 2005: A study of extratropical transition in the western North Atlantic Ocean, 1963–1996. *Atmos.–Ocean,* **43,** 173–191.

Foley, G., and B. Hanstrum, 1994: The capture of tropical cyclones by cold fronts off the west coast of Australia. *Wea. Forecasting,* **9,** 577–590.

Gyakum, J., 2003: The extratropical transformation: A scientific challenge. *Atmosphere–Ocean Interactions*, W. Perrie, Ed., Vol. 1, WIT Press, 47–81.

Harr, P., and R. Elsberry, 2000: Extratropical transition of tropical cyclones over the western North Pacific. Part I: Evolution of structural characteristics during the transition process. *Mon. Wea. Rev.,* **128,** 2613–2633.

——, ——, and T. Hogan, 2000: Extratropical transition of tropical cyclones over the western North Pacific. Part II: The impact of midlatitude circulation characteristics. *Mon. Wea. Rev.,* **128,** 2634–2653.

Hart, R. E., and J. Evans, 2001: A climatology of the extratropical transition of Atlantic tropical cyclones. *J. Climate,* **14,** 547–564.

——, ——, and C. Evans, 2006: Synoptic composites of the extratropical transition life cycle of North Atlantic tropical cyclones: Factors determining posttransition evolution. *Mon. Wea. Rev.,* **134,** 553–578.

Hoskins, B., M. McIntyre, and A. Robertson, 1985: On the use and significance of isentropic potential vorticity maps. *Quart. J. Roy. Meteor. Soc.,* **111,** 877–946.

Jones, S., and Coauthors, 2003: The extratropical transition of tropical cyclones: Forecast challenges, current understanding and future directions. *Wea. Forecasting,* **18,** 1052–1092.

Kalnay, E., and Coauthors, 1996: The NCEP/NCAR 40-Year Reanalysis Project. *Bull. Amer. Meteor. Soc.,* **77,** 437–471.

Klein, P., P. Harr, and R. Elsberry, 2000: Extratropical transition of western North Pacific tropical cyclones: An overview and conceptual model of the transformation stage. *Wea. Forecasting,* **15,** 373–395.

——, ——, and ——, 2002: Extratropical transition of western North Pacific tropical cyclones: An overview and conceptual model of the transformation stage. *Mon. Wea. Rev.,* **130,** 2240–2259.

Koch, S., M. DesJardins, and P. Kocin, 1983: An interactive Barnes objective map analysis scheme for use with satellite and conventional data. *J. Appl. Meteor.,* **22,** 1487–1503.

Ma, S., H. Ritchie, J. Gyakum, J. Abraham, C. Fogarty, and R. McTaggart-Cowan, 2003: A study of the extratropical reintensification of former Hurricane Earl using Canadian Meteorological Centre regional analyses and ensemble forecasts. *Mon. Wea. Rev.,* **131,** 1342–1359.

Matano, H., and M. Sekioka, 1971a: On the synoptic structure of Typhoon Cora, 1969, as the compound system of tropical and extratropical cyclones. *J. Meteor. Soc. Japan,* **49,** 282–294.

——, and ——, 1971b: Some aspects of extratropical transformation of a tropical cyclone. *J. Meteor. Soc. Japan,* **49,** 736–743.

Matano, J., 1958: On the synoptic structure of Hurricane Hazel, 1954, over the eastern United States. *J. Meteor. Soc. Japan,* **36,** 23–31.

McTaggart-Cowan, R., J. Gyakum, and M. Yau, 2003: The influence of the downstream state on extratropical transition: Hurricane Earl (1998) case study. *Mon. Wea. Rev.,* **131,** 1910–1929.

——, ——, and ——, 2004a: The impact of tropical remnants on extratropical cyclogenesis: Case study of Hurricanes Danielle and Earl (1998). *Mon. Wea. Rev.,* **132,** 1933–1951.

——, ——, and ——, 2004b: Reply. *Mon. Wea. Rev.,* **132,** 2514–2519.

Mesinger, F., and Coauthors, 2006: North American Regional Reanalysis. *Bull. Amer. Meteor. Soc.,* **87,** 343–360.

Morgan, M., and J. Nielsen-Gammon, 1998: Using tropopause maps to diagnose midlatitude weather systems. *Mon. Wea. Rev.,* **126,** 2555–2579.

Palmén, E., 1958: Vertical circulation and release of kinetic energy during the development of Hurricane Hazel into an extratropical storm. *Tellus,* **10,** 1–23.

Ritchie, E. A., and R. L. Elsberry, 2003: Simulations of the extratropical transition of tropical cyclones: Contributions by the midlatitude upper-level trough to reintensification. *Mon. Wea. Rev.,* **131,** 2112–2128.

——, and ——, 2007: Simulations of the extratropical transition of tropical cyclones: Phasing between the upper-level trough and tropical cyclones. *Mon. Wea. Rev.,* **135,** 862–876.

Thorncroft, C., and S. Jones, 2000: The extratropical transition of Hurricanes Felix and Iris in 1995. *Mon. Wea. Rev.,* **128,** 947–972.

Trenberth, K. E., 1978: On the interpretation of the diagnostic quasi-geostrophic omega equation. *Mon. Wea. Rev.,* **106,** 131–137.

Weese, S., 2003: A reanalysis of Hurricane Hazel (1954). M.S. thesis, Dept. of Atmospheric and Oceanic Sciences, McGill University, 123 pp.